Supporting Information

A mitochondria-targeting photothermogenic nanozyme for MRI-guided mild photothermal therapy

Kangqiang Qiu,[‡a,b] Jinquan Wang,[‡c] Thomas W. Rees,[a] Liangnian Ji,[a] Qianling Zhang*[b] and Hui Chao*[a,b]

[a] *MOE Key Laboratory of Bioinorganic and Synthetic Chemistry, School of Chemistry, Sun Yat-Sen University, Guangzhou 510275, P. R. China. E-mail: ceschh@mail.sysu.edu.cn (H. Chao)*

[b] *College of Chemistry and Environmental Engineering, Shenzhen University, Shenzhen, 518055, P. R. China. E-mail: zhql@szu.edu.cn (Q. Zhang)*

[c] *Guangdong Provincial Key Laboratory of Biotechnology Candidate Drug Research, Guangdong Pharmaceutical University, Guangzhou, 510006, China.*

‡ These authors contributed equally to this work.

Table of Contents

Experimental Section

Materials

Unless otherwise specified, all commercial reagents were used without further purification. $IrCl_3$, aniline, 2-phenylpyridine (ppy), 3,4-dihydroxybenzaldehyde, 3-(4,5-dimethylthiazol-2-yl)-2,5-diphenyltetrazolium bromide (MTT), 5,5',6,6'-tetrachloro-1,1'-3,3'-tretraethyl-benzimidazolylcarbocyanine iodide (JC-1), 2,7-dichlorodihydro-fluorescein diacetate (DCFH-DA), 5,5-dimethyl-1-pyrroline-*N*-oxide (DMPO), $Fe(acac)_3$, benzyl ether, methylene blue and oleylamine were purchased from Sigma. The live/dead cell imaging kit and hydroxyl radical sensor (HPF) were purchased from Thermo Fisher Scientific. 1,10-phenanthroline-5,6-dione and $[Ir(ppy)_2Cl]_2$ were prepared according to literature methods.[1,2]

General instruments

^1H NMR spectra were performed on a nuclear magnetic resonance spectrometer (AVANCE III 400 MHz). Electrospray ionization mass spectra (ESI-MS) were obtained by an LCQ system (Finnigan MAT, USA). Microanalyses (C, H and N) were determined by a Perkin-Elmer 240Q elemental analyzer. Tetramethylsilane (TMS) was used as reference for the chemical shifts in the ^1H NMR spectra. The UV-Vis-NIR spectra were obtained with a spectrophotometer (Perkin-Elmer Lambda 850) at 25 °C. The morphology and the microstructure of the particles were characterized by 300 kv transmission electron microscopy (TEM, Tecnai^{TM} G2 F30, FEI). The X-ray photoelectron spectroscopy (XPS, ESCALAB 250, Thermo-VG Scientific) with 200 W Al KR radiated in twin anode. Infrared spectra were obtained with a Nicolet 170SX-FTIR spectrophotometer and KBr discs. X-ray diffraction (XRD) measurement was recorded using a X-ray powder diffractometer (SmartLab, Rigaku Co.) and the diffraction peaks were indexed to the typical cubic structure of Fe_3O_4 (JCPDS. 01-1111).[3] Thermogravimetric analysis (TGA) spectrum was obtained by a thermogravimetric instruments (TG 209 F3 Tarsus, NETZSCH). The room-temperature magnetic properties of the particles and magnetic resonance imaging were measured on a MesoMR21-060H-I imaging instrument (Shanghai Niumag Corp.).

Digesting dried **Ir@Fe_3O_4 NPs** in concentrated HNO_3, Fe content and Ir content were determined by inductively coupled plasma mass spectrometry (ICP-MS, Thermo Elemental Co., Ltd.). Dynamic light scattering and zeta potential experiments were performed using dynamic laser light scattering equipment (BI-PALS03030131, Brookhaven Inst. Corp.). The bio-TEM image was obtained with a JEM100CX electron microscope. Milli-Q water was obtained from a Milli-Q system of Millipore Company (Boston, MA, USA). A diode laser (808 nm) from Hi-Tech Optoelectronics Co., Ltd. (Beijing, China) was used in this study. Electron spin resonance (ESR) spectra were measured by Bruker Model A300 spectrometer at 298 K and DMPO was elected as a spin trap for the hydroxyl radical.[4] The *n*-octanol/water partition coefficient (log *P*) was measured by a spectrophotometer (Perkin-Elmer Lambda 850) as the reported method.[5] Origin 8 was used to process all data.

Synthesis of 4-(1-phenyl-1*H*-imidazo[4,5-*f*][1,10]phenanthrolin-2-yl)benzene-1,2-diol (L)

A mixture of 1,10-phenanthroline-5,6-dione (0.210 g, 1 mmol), ammonium acetate (1.540 g, 20 mmol), 3,4-dihydroxybenzaldehyde (0.138g, 1 mmol), glacial acetic acid (10 mL) and aniline (0.093g, 1 mmol) was refluxed under argon for 24 h. The reaction mixture was then cooled to room temperature and poured into water (20 mL). The solution was neutralized with a 25% NH_3 solution. To the solution, dichloromethane (DCM) was added and the organic materials were extracted in the organic layer, from which rotary evaporation afforded the green crude product. The crude product was then purified using column chromatography (DCM/ethanol) to obtain a white compound (yield = 52%). ^{1}H NMR (400 MHz, DMSO-d_6, δ) 9.08 (d, J = 3.9 Hz, 1H), 8.99 (d, J = 8.1 Hz, 1H), 8.93 (d, J = 3.9 Hz, 1H), 7.87 (dd, J = 8.0, 4.2 Hz, 1H), 7.72 (s, 5H), 7.46 (dd, J = 8.3, 4.3 Hz, 1H), 7.30 (d, J = 8.4 Hz, 1H), 7.16 (s, 1H), 6.75 (d, J = 9.4 Hz, 1H), 6.64 (d, J = 8.3 Hz, 1H). ESI-MS *m*/*z*: 405.05 $[M + H]^+$, 427.05 $[M + Na]^+$, 459.00 $[M + Na + CH_3OH]^+$. Anal. Calcd for $C_{25}H_{16}N_4O_2$: C 74.25, H 3.99, N 13.85; found: C 73.88, H 4.01, N 13.78.

Synthesis of $[Ir(ppy)_2L]PF_6$ (Ir)

The ligand **L** (0.081 g, 0.2 mmol) and $[Ir(ppy)_2Cl]_2$ (0.107 g, 0.1 mmol) were placed in a 25 mL round bottomed flask with 7 mL of dimethyl formamide (DMF). The mixture was heated at 140 °C for 12 h under argon. After 12 h, the cooled reaction mixture was diluted with water (25 mL). Saturated aqueous KPF_6 solution was added under vigorous stirring, and filtered. The yellow solid was collected and washed with small amounts of water and diethyl ether, then dried under vacuum. The pure iridium complex was obtained by recrystallization (yield = 48%). ^{1}H NMR (400 MHz, DMSO-d_6, δ) 9.52 (s, 1H), 9.29 (d, J = 8.2 Hz, 1H), 9.22 (s, 1H), 8.31-8.22 (m, 3H), 8.14 (dd, J = 7.9, 5.3 Hz, 1H), 8.06 (d, J = 4.9 Hz, 1H), 7.99-7.87 (m, 4H), 7.76 (s, 6H), 7.53-7.42 (m, 3H), 7.18 (s, 1H), 7.10-6.92 (m, 6H), 6.81 (d, J = 9.4 Hz, 1H), 6.68 (d, J = 8.4 Hz, 1H), 6.29 (dd, J = 13.4, 7.5 Hz, 2H). ESI-MS m/z: 905.00 $[M - PF_6^-]^+$. Anal. Calcd for $C_{47}H_{32}F_6IrN_6O_2P$: C 53.76, H 3.07, N 8.00; found: C 53.51, H 3.08, N 7.96.

Synthesis of Fe_3O_4 NPs

The synthesis of Fe_3O_4 NPs was used the reported method.[6,7] $Fe(acac)_3$ (0.706 g, 2mmol) was dissolved in a mixture of benzyl ether (10 mL) and oleyl amine (10 mL). The above mixture solution was dehydrated at 110 °C for 1 h under a flow of argon, and quickly heated to 300 °C and kept at this temperature for 2 h under a blanket of argon. The black-brown mixture was cooled to room temperature by removing the heat source. Under ambient conditions, ethanol (40 mL) was added to the mixture, and a black material was precipitated and separated *via* centrifugation (8000 rpm, 10 min). The black product was dissolved in hexane. Centrifugation (6000 rpm, 10 min) was applied to remove any undispersed residue. The product was then precipitated with ethanol, centrifuged (8000 rpm, 10 min) to remove the solvent, and re-dispersed into hexane.

Synthesis of Ir@Fe_3O_4 NPs

Under ambient conditions, **Ir** (20 mg) was dissolved in dichloromethane (5 mL), and then Fe_3O_4 NPs (10 mg) in 1 mL dichloromethane were added. The mixture was stirred overnight at room temperature. Centrifugation (6000 rpm, 10 min) was applied to remove any

undispersed residue. The particles were precipitated and separated using a magnet. The solvent was decanted and the precipitate was washed with dichloromethane and separated again using a magnet to remove excess **Ir** before drying under argon.

The formation of **Ir@Fe_3O_4 NPs** was characterized by transmission electron microscopy (TEM), infrared spectroscopy (IR), X-ray photoelectron spectroscopy (XPS), thermogravimetric analysis (TGA), X-ray diffraction (XRD), and inductively coupled plasma mass spectrometry (ICP-MS).

Photothermal performance in solution

To investigate the photothermal conversion effect, a series of solutions of **Ir@Fe_3O_4 NPs** (0.0, 0.1, 0.2, 0.4 and 0.6 mg mL^{-1}) in pH 8.0 PBS were irradiated by an 808 nm laser (1.0 W cm^{-2}, 6 min). As a control, the temperatures of Ir(III) complex solution irradiated by the same laser were measured. To verify the function of NIR laser power density, the solution of **Ir@Fe_3O_4 NPs** (0.2 mg mL^{-1}) in pH 8.0 PBS was irradiated with different NIR power densities (1.0, 1.5, 2.0 and 2.5 W cm^{-2}). The temperature changes were measured with a thermal camera (MAG32, Magnity Electronics, Thermal Imaging Expert) over 6 min. All the experiments were conducted at room temperature.

Study of photothermogenic catalysis of Ir@Fe_3O_4 NPs

All the assays were performed in PBS at pH 8.0. For the solution with particles, centrifugation at 14000 rpm for 5 min was conducted before measurements. The concentrations of **Ir@Fe_3O_4 NPs**, H_2O_2 and **Ir** were 0.2 mg mL^{-1}, 10 mM, and 20 μM, respectively.

The ability of **Ir@Fe_3O_4 NPs** to catalyse the production of •OH was detected by the hydroxyl radical sensor HPF and an electron spin resonance (ESR) assay at 25 °C.[8,9] The fluorescence of the hydroxyl radical sensor HPF (5 uM) is very weak, but becomes strong after the reaction with hydroxyl radical. Classical fluorescent method were used to meausure the intensity changes. For ESR assay, 5,5-dimetryl-1-pyrroline-*N*-oxide (DMPO, 450 mM) was used as a spin trapping agent for •OH. ESR measurement were carried out by using

three settings to detect the spin adduct •OH-DMPO: 20 mW microwave power, 100 G scan range, and 1 G field modulation.

The temperature-dependence of catalysis for **Ir@Fe_3O_4 NPs** to generate •OH was confirmed by the ESR assay and methylene blue (MB, 20 μM) decoloration experiment at 25 °C, 37 °C and 42 °C, with heating by photothermal conversion. The colorimetric method was used to measure the absorbance of MB.[10]

HeLa cells culture conditions

HeLa cells were maintained as monolayer cultures in high-glucose Dulbecco's modified eagle medium (DMEM, Gibco, USA) supplemented with 10% Fetal Bovine Serum (FBS) and were cultured at 37 °C in humidified atmosphere under 5% CO_2.

MTT assay

After HeLa cells were seeded in triplicate into 96-well plates for 24 h, the cells were treated with increasing concentration of **Ir** and **Ir@Fe_3O_4 NPs** for different times. To stain the viable cells, 20 μL of MTT (5 mg mL^{-1}) was added to each well. After 4 h, the media was aspirated and 200 μL of DMSO was added per well. The optical density of each well was measured by a Tecan Infinite M200 monochromatic multifunction microplate reader at 595 nm and the cell survival rate of the well without **Ir** and **Ir@Fe_3O_4 NPs** addition was considered to be 100%.

ICP-MS analysis

For the uptake studies, exponentially growing HeLa cells were harvested, and the resulting single-cell suspension was plated into 10 cm tissue culture plates (Costar). After 24 h at 37 °C, the cells were incubated with **Ir** and **Ir@Fe_3O_4 NPs** (5 μM for **Ir** and 0.2 mg mL^{-1} for **Ir@Fe_3O_4 NPs**) for 4 h at 37 °C. The cells were rinsed with PBS, detached with trypsin, counted and divided into three portions. The nuclei, the cytoplasm, and the mitochondria were extracted following the manufacturer's' protocol of the nucleus extraction kit, the cytoplasm extraction kit, and the mitochondrial extraction kit (Pierce and

Thermo), respectively. The samples were digested with 60% HNO_3 at RT for one day. Each sample was diluted with Milli-Q H_2O to obtain 2% HNO_3 sample solutions. The iridium content was measured using ICP-MS for its exogenesis.

Bio-TEM imaging analysis

Treated with 0.2 mg mL^{-1} **Ir@Fe_3O_4 NPs** for 2 h and 4 h, HeLa cells were rinsed with PBS, detached with trypsin, and obtained by centrifuge. For bio-TEM imaging analysis, cells were fixed in 0.1 M PBS containing 2.5% glutaraldehyde and 4% paraformaldehyde for 1 h, rinsed with distilled water, stained with 0.5% uranyl acetate for 1 h, dehydrated in a graded series of ethanol (30, 60, 70, 90 and 100%), and embedded in epoxy resin. The resin was polymerized at 60 °C for 48 h. Ultrathin sections (50-75 nm) obtained with a LKB ultramicrotome were stained with 2% aqueous uranyl acetate and 2% aqueous lead citrate. Bio-TEM images were obtained with a JEM100CX electron microscope.

Photothermal performance in HeLa cells

Treated with 0.0 and 0.2 mg mL^{-1} of **Ir@Fe_3O_4 NPs** for 4 h, HeLa cells were irradiated by an 808 nm laser at 1.0 W cm^{-2} for 4 min and the temperatures were monitored by a thermal camera.

Cell imaging

HeLa cells were plated onto 35 mm glass bottom dishes (Corning) and allowed to adhere for 24 h. The cells were set to four control groups and one treatment group. The control groups were: without treatment, NIR, 42 °C and **Ir@Fe_3O_4 NPs**. For NIR, the cells were irradiated by an 808 nm laser at 1.0 W cm^{-2} for 15 min, the same irradiation dose treatment as the treatment group. For 42 °C, the cells were irradiated by an 808 nm laser at 3.0 W cm^{-2} for 15 min and a thermal camera was used to control the temperature between 42 ± 1 °C, the same temperature treatment as the treatment group. For **Ir@Fe_3O_4 NPs**, the cells were treated with **Ir@Fe_3O_4 NPs** (0.2 mg mL^{-1}) for 4 h, the same **Ir@Fe_3O_4 NPs** concentration treatment as the treatment group. For the treatment group (**Ir@Fe_3O_4 NPs** + NIR), the cells

were treated with the **Ir@Fe_3O_4 NPs** (0.2 mg mL^{-1}) for 4 h and irradiated by an 808 nm laser (1.0 W cm^{-2}, 15 min) at a temperature between 42 ± 1 °C, which was monitored by a thermal camera.

For detecting reactive oxygen species (ROS), after the treatment of 0.2 mg mL^{-1} of the **Ir@Fe_3O_4 NPs** for 4 h, the five groups were incubated with DCFH-DA (10 μM, λ_{ex} = 488 nm, λ_{em} = 500-520 nm) for 0.5 h before irradiation. Cell imaging was performed using an inverted fluorescence microscope (Zeiss Axio Observer D1, Germany) after irradiation.

For detecting $^{\bullet}OH$, after the treatment of 0.2 mg mL^{-1} of the **Ir@Fe_3O_4 NPs** for 4 h, the five groups were incubated with HPF (5 μM, λ_{ex} = 488 nm, λ_{em} = 500-520 nm) for 0.5 h before the irradiation. Cell imaging was performed using a Zeiss LSM 710 NLO confocal microscope (63×/NA 1.4 oil immersion objective) after irradiation.

For analysis of the mitochondrial membrane potential, after the treatment of 0.2 mg mL^{-1} of the **Ir@Fe_3O_4 NPs** for 4 h, the five groups were stained with JC-1 (10 μM. For J-monomer, λ_{ex} = 488 nm, λ_{em} = 500-520 nm; for J-aggregates, λ_{ex} = 543 nm, λ_{em} = 590-630 nm.) for 0.5 h before the irradiation. Cell imaging was performed using an inverted fluorescence microscope (Zeiss Axio Observer D1, Germany) after irradiation.

For live/dead cell deteting, after the conducts for the five groups, LIVE/DEAD cell imaging kit (Calcein AM for live cells, λ_{ex} = 488 nm, λ_{em} = 500-520 nm; PI for dead cells, λ_{ex} = 543 nm, λ_{em} = 590-630 nm. Thermo Fisher Scientific) was used to stain the cells for 0.5 h. Cell imaging was performed using an inverted fluorescence microscope (Zeiss Axio Observer D1, Germany) after the media was replaced.

T_2-weighted MRI *in vivo*

T_2-weighted imaging was performed using a MesoMR21-060H-I imaging instrument (Shanghai Niumag Corp.). A tumor-bearing mouse was anaesthetized with ketamine (10 mL kg^{-1}). Imaging was performed before, and after intratumoral injection of **Ir@Fe_3O_4 NPs** at a dose of 100 μL (2.0 mg mL^{-1}). The instrumental parameters were set as follows: 0.5 T magnet, section thickness = 3.0 mm, TE = 45 ms, TR = 1600 ms, and number of scans (NS) = 6.

In vivo therapy

BALB/c-(nu/nu) female nude mice aged 4-5 weeks were purchased and bred in the Traditional Chinese Medicine and Marine Medicine Laboratory, School of Life Sciences, Sun Yat-Sen University. All experimental protocols were approved by the Sun Yat-Sen University Animal Care and Use Committee. HeLa xenograft tumors were established by inoculating 2×10^6 cells via subcutaneous injection (s.c.) into four BALB/c-(nu/nu) female nude mice. When the tumor volumes reached approximately 150 mm^3, the well-grown tumors were cut into 1 mm^3 fragments, and the fragments were transplanted (s.c.) into the other nude mice. When the tumor volumes of the other mice reached approximately 120 mm^3, the nude mice were randomly allocated into five groups (six mice per group) before the experiments. The groups were set to four control groups and one treatment group. The control groups were control without any treatments, NIR, 42 °C and **Ir@Fe_3O_4 NPs**, respectively.

The photothermal therapy process was as follows:

Group 1 (Control): mice were intratumorally injected with the same volume (100 μL) of physiological saline solution;

Group 2 (NIR): mice were intratumorally injected with the same volume (100 μL) of physiological saline solution and were irradiated by an 808 nm laser (1.0 W cm^{-2}, 30 min);

Group 3 (42 °C): mice were intratumorally injected with the same volume (100 μL) of physiological saline solution and irradiated by an 808 nm laser (3.0 W cm^{-2}, 30 min) at a temperature between 42 ± 1 °C, which was monitored by a thermal camera;

Group 4 (**Ir@Fe_3O_4 NPs**): mice were intratumorally injected with the **Ir@Fe_3O_4 NPs** (100 μL of 2.0 mg mL^{-1} solution);

Group 5 (**Ir@Fe_3O_4 NPs** + NIR): mice were intratumorally injected with the **Ir@Fe_3O_4 NPs** (100 μL of 2.0 mg mL^{-1} solution). After 6 h injection, mice were irradiated by an 808 nm laser (1.0 W cm^{-2}, 30 min) at a temperature between 42 ± 1 °C, which was monitored by a thermal camera.

After 6 days, the same treatments were performed to all groups again. A thermal camera was used to control the temperature between 42 ± 1°C. The mice were anesthetized by Gas Anesthesia Systems (XGI-8, XENOGEN, USA). After the irradiation (day 0), the tumor

sizes were measured using a caliper every 3 days. The mice with tumors were photographed with a digital color camera at day 0, day 5, and day 15.

Histological examination

At the end of the photothermal therapy *in vivo*, all the mice of the five groups were sacrificed and the tumors and the organs including liver, kidney, spleen, heart, lung, brain, intestine and ovary were resected. After immersion in 4% paraformaldehyde at 4 °C, the sections of the organs were obtained as paraffin-embedded samples and stained with H&E. Deep blue-purple hematoxylin and pink Eosin stain were used for nucleic acids and proteins, respectively. An Olympus microscope was used to observe the tissue structure and cell state of the sections.

Statistical analysis

Data were presented as mean result ± standard deviation, and significance was assessed with each experiment was subjected to statistical analysis by the Student–Newmann–Keuls analysis of variance and with the *t*-test for grouped data. Differences were considered significant at *P* less than 0.05.

References

[1] M. Yamada, Y. Tanaka, Y. Yoshimoto, S. Kuroda and I. Shimao, *Bull. Chem. Soc. Jpn.*, 1992, **65**, 1006.

[2] D. L. Ma, H. Z. He, K. H. Leung, D. S. H. Chan and C. H. Leung, *Angew. Chem. Int. Ed.*, 2013, **52**, 7666.

[3] Z. Zhu, Z. Wang, Y. Hao, C. Zhu, Y. Jiao, H. Chen, Y.-M. Wang, J. Yan, Z. Guo and X. Wang, *Chem. Sci.*, 2016, **7**, 2864.

[4] H. Huang, B. Yu, P. Zhang, J. Huang, Y. Chen, G. Gasser, L. Ji and H. Chao, *Angew. Chem. Int. Ed.*, 2015, **54**, 14049.

[5] X. Zhang, C. Wang, Z. Han and Y. Xiao, *ACS Appl. Mater. Interfaces*, 2014, **6**, 21669.

[6] S. Sun and H. Zeng, *J. Am. Chem. Soc.*, 2002, **124**, 8204.

[7] S. Sun, H. Zeng, D. B. Robinson, S. Raoux, P. M. Rice, S. X. Wang and G. Li, *J. Am. Chem. Soc.*, 2004, **126**, 273.

[8] H. P. Indo, M. Davidson, H.-C. Yen, S. Suenaga, K. Tomita, T. Nishii, M. Higuchi, Y. Koga, T. Ozawa and H. J. Majima, *Mitochondrion*, 2007, **7**, 106.

[9] M. A. Voinov, J. O. Pagan, E. Morrison, T. I. Smirnova and A. I. Smirnov, *J. Am. Chem. Soc.*, 2011, **133**, 35.

[10] C. Zhang, W. Bu, D. Ni, S. Zhang, Q. Li, Z. Yao, J. Zhang, H. Yao, Z. Wang and J. Shi, *Angew. Chem. Int. Ed.*, 2016, **55**, 2101.

Supporting Figures

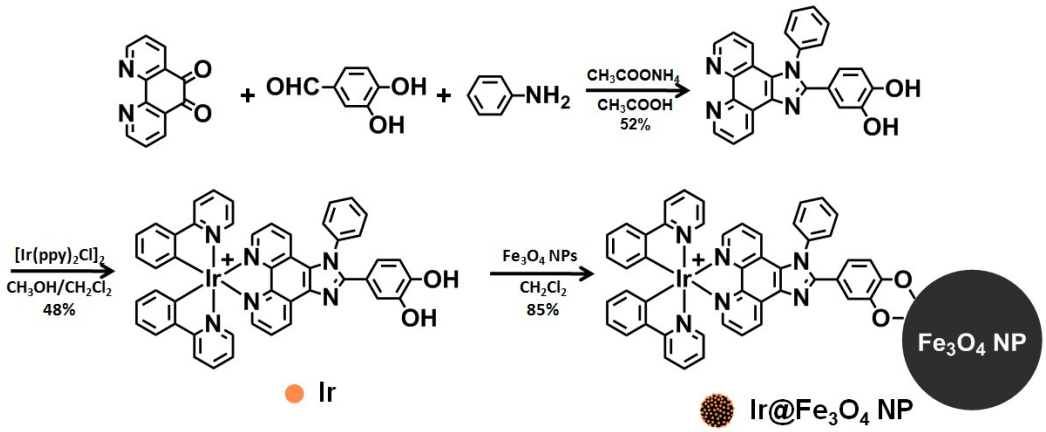

Scheme S1 Synthetic route to **Ir@Fe_3O_4 NPs**.

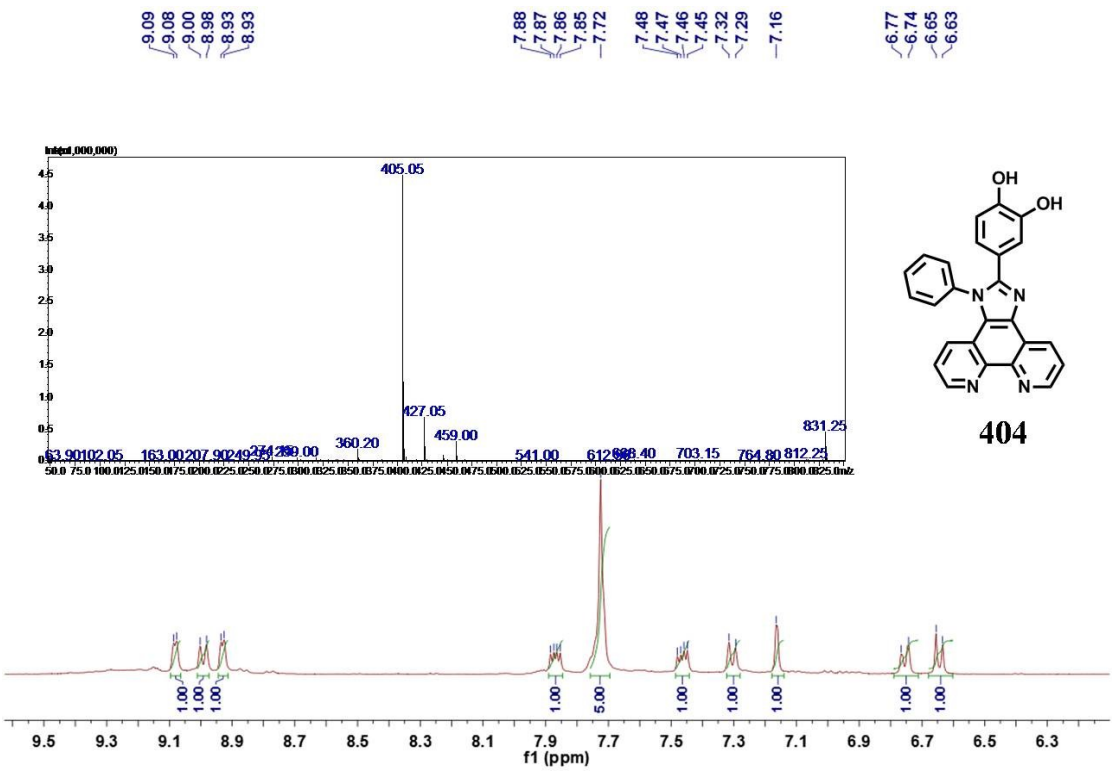

Fig. S1 The ESI-MS spectrum and ^{1}H NMR spectrum of ligand **L**.

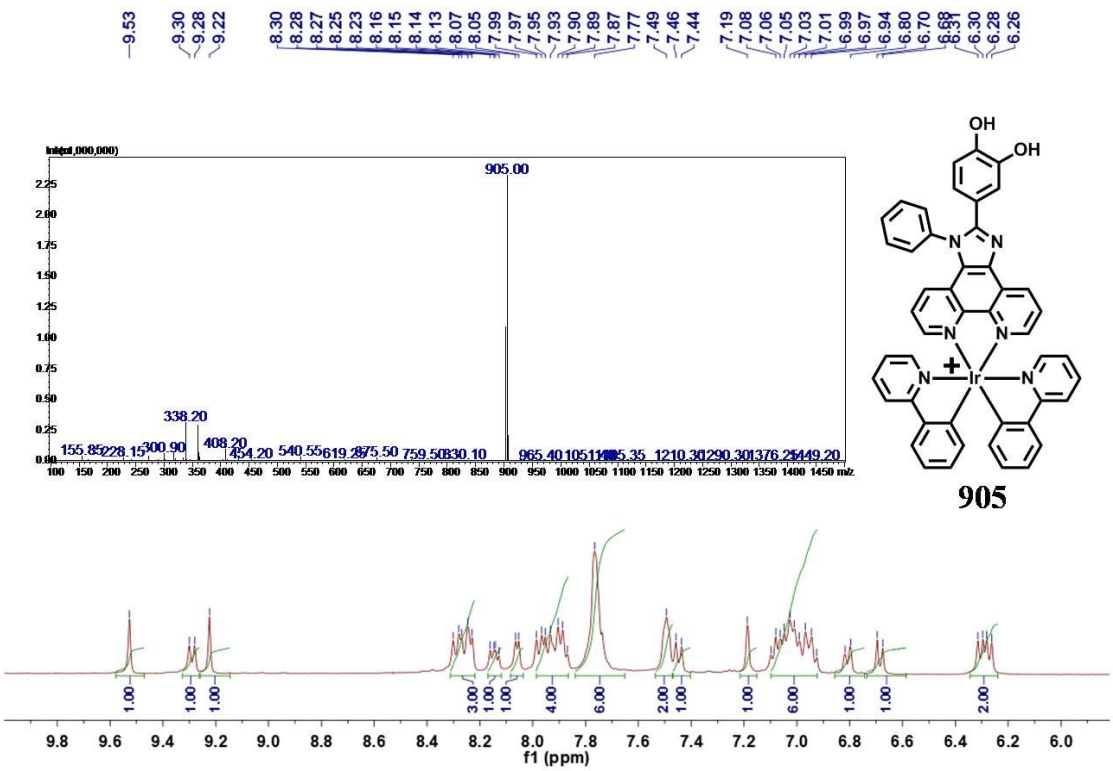

Fig. S2 The ESI-MS spectrum and ^{1}H NMR spectrum of the complex **Ir**.

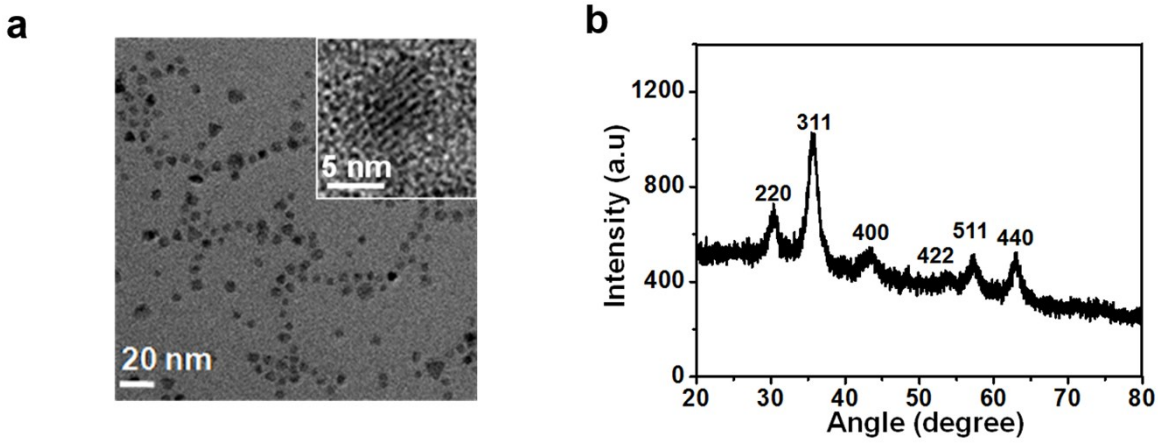

Fig. S3 (a) TEM image of **Ir@Fe_3O_4 NPs**. Inset: high-resolution TEM image. (b) X-ray diffraction pattern of **Ir@Fe_3O_4 NPs**.

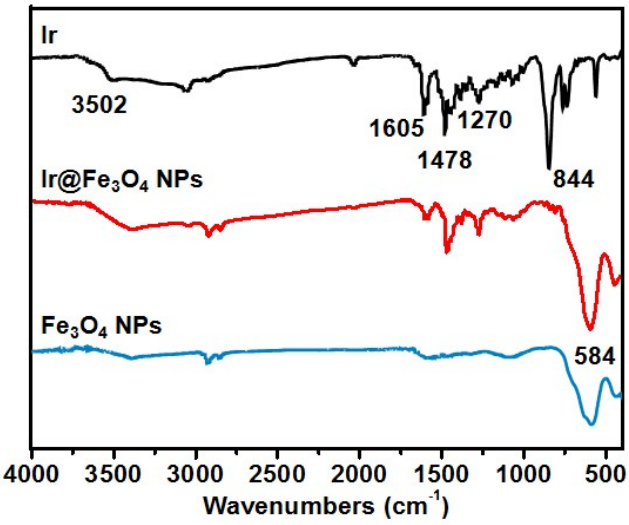

Fig. S4 IR spectra of **Ir**, Fe_3O_4 NPs and **Ir@Fe_3O_4 NPs**.

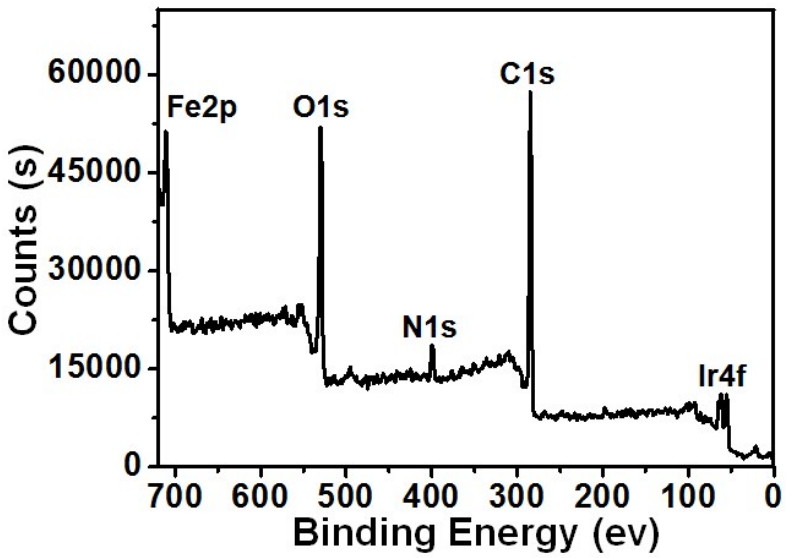

Fig. S5 XPS spectrum of **Ir@Fe_3O_4 NPs**.

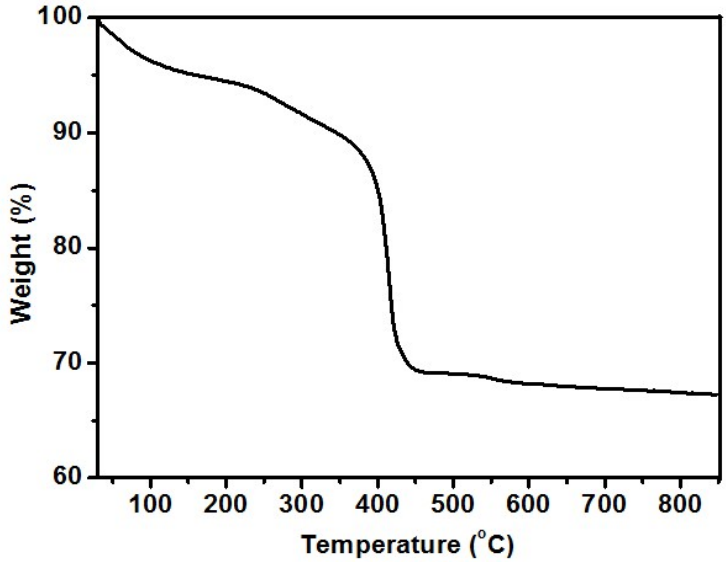

Fig. S6 TGA spectrum of **Ir@Fe_3O_4 NPs**.

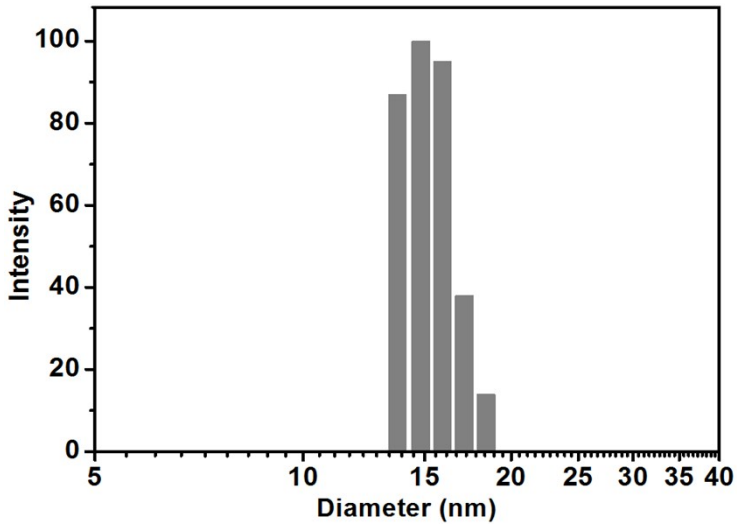

Fig. S7 Hydrodynamic diameter of **Ir@Fe_3O_4 NPs** in PBS (pH 8.0).

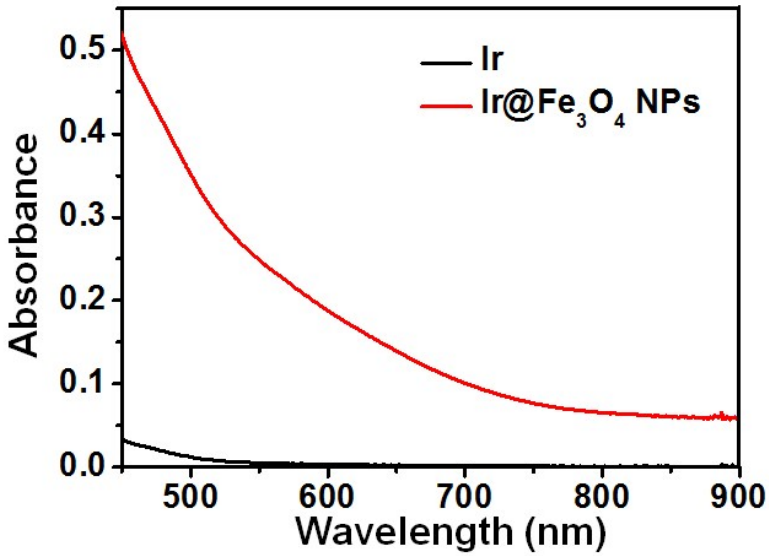

Fig. S8 UV-Vis-NIR absorption spectra of **Ir** and **Ir@Fe_3O_4 NPs**.

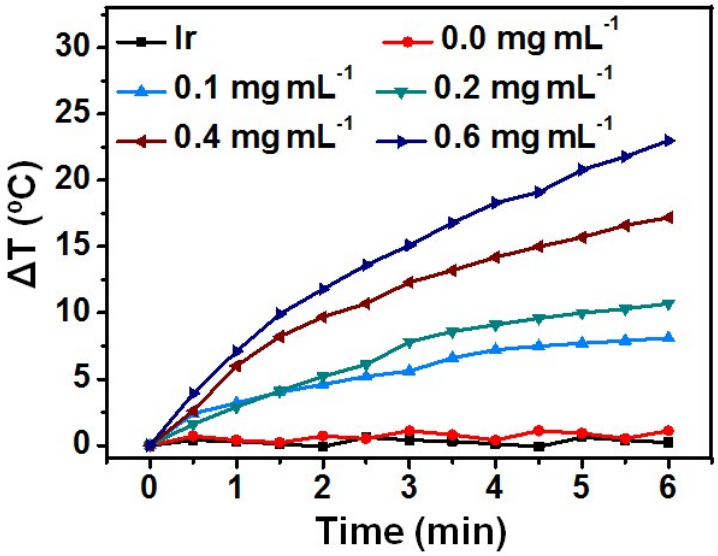

Fig. S9 Temperature curve at different concentrations of **Ir@Fe_3O_4 NPs** and **Ir** with irradiation at 1.0 W cm^{-2}.

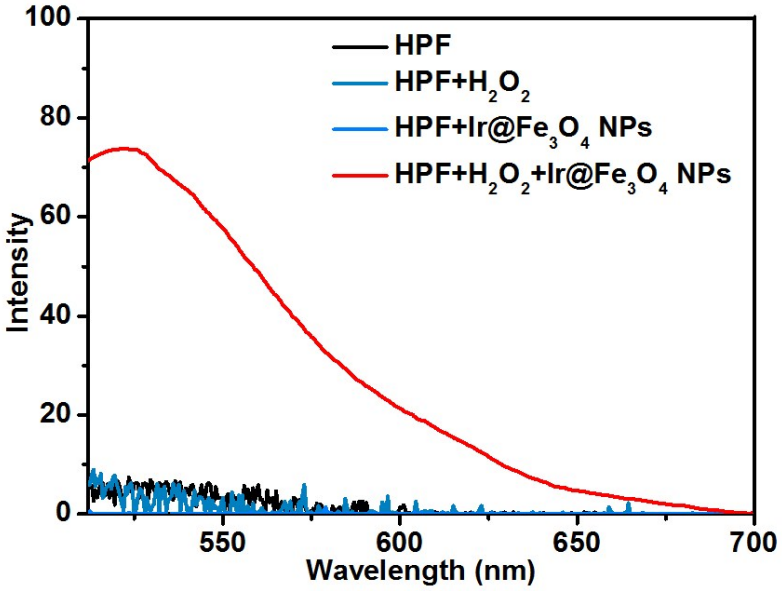

Fig. S10 The emissive spectra of HPF (5 μM) in PBS (pH 8.0).

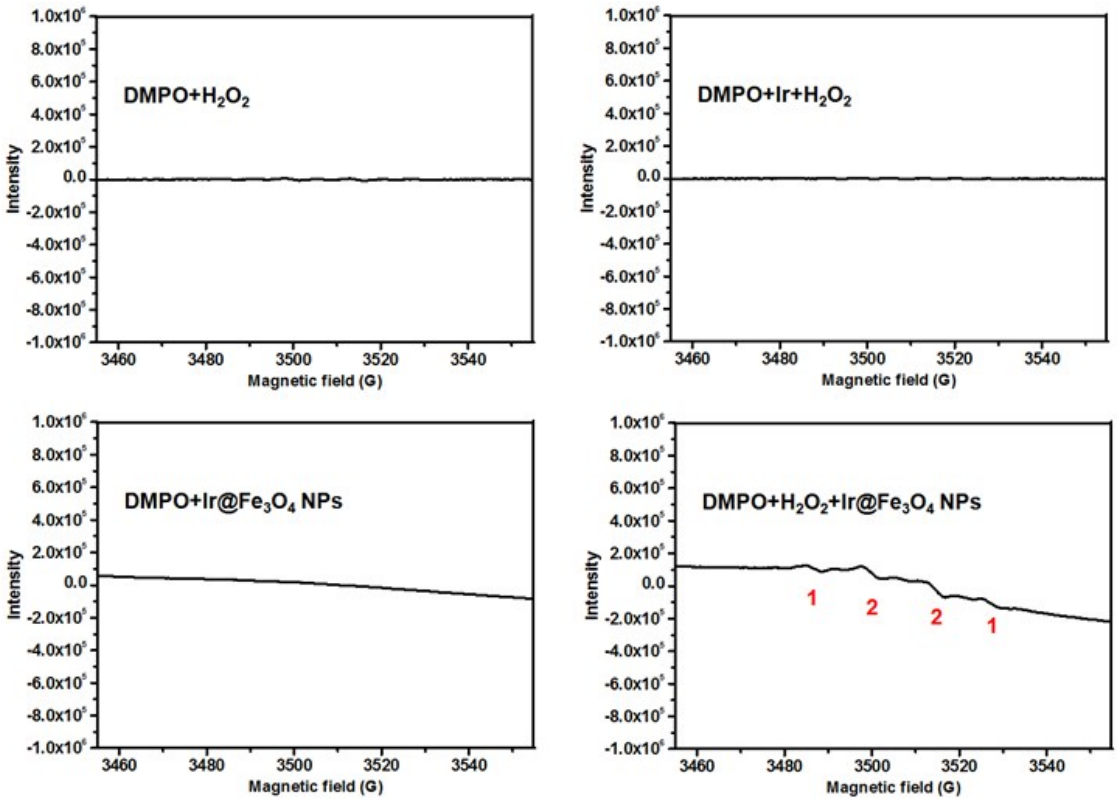

Fig. S11 The ESR spectra of DMPO in PBS (pH 8.0). Without centrifugation, the background of the Fe_3O_4 NPs was found in the ESR spectra.

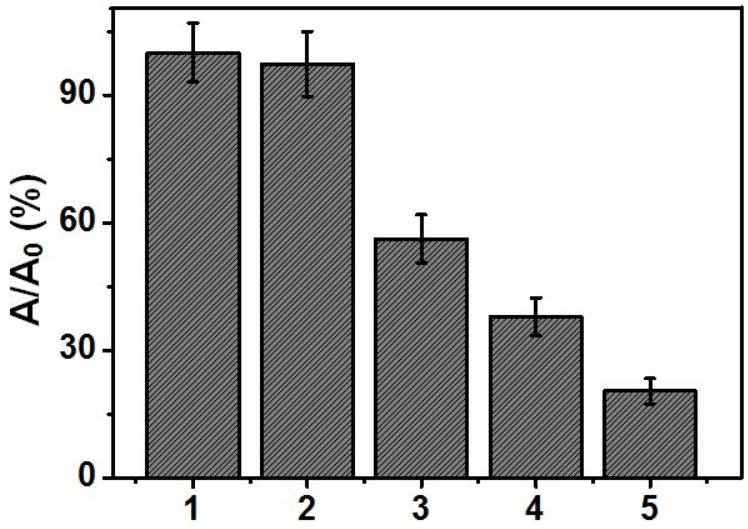

Fig. S12 Colorimetric analysis of catalysis for MB decolourisation of **Ir@Fe_3O_4 NPs** at different temperatures. 1. MB; 2. MB + H_2O_2 + 25 °C; 3. MB + H_2O_2 + **Ir@Fe_3O_4 NPs** + 25 °C; 4. MB + H_2O_2 + **Ir@Fe_3O_4 NPs** + 37 °C; 5. MB + H_2O_2 + **Ir@Fe_3O_4 NPs** + 42 °C.

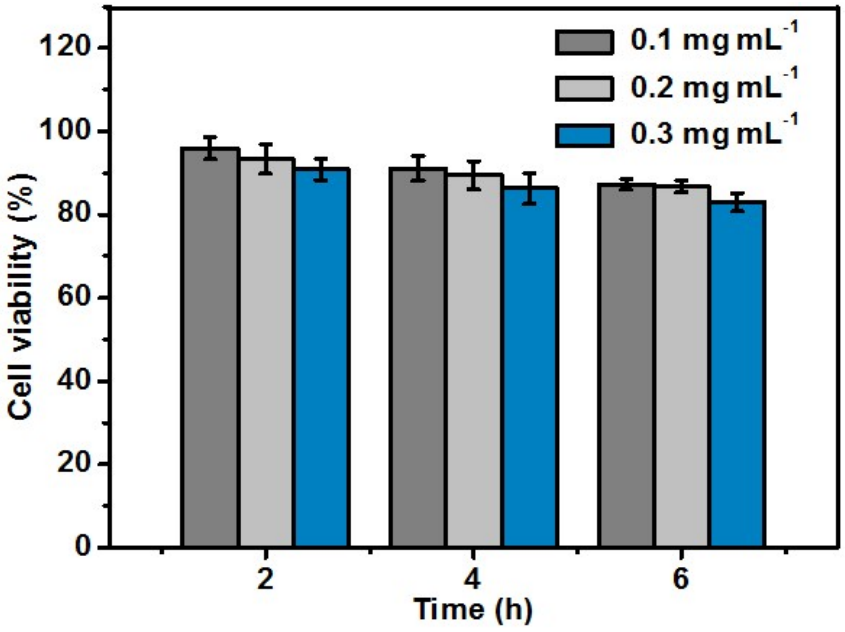

Fig. S13 Cell viability of HeLa cells incubated with different concentrations of **Ir@Fe_3O_4 NPs** for different times.

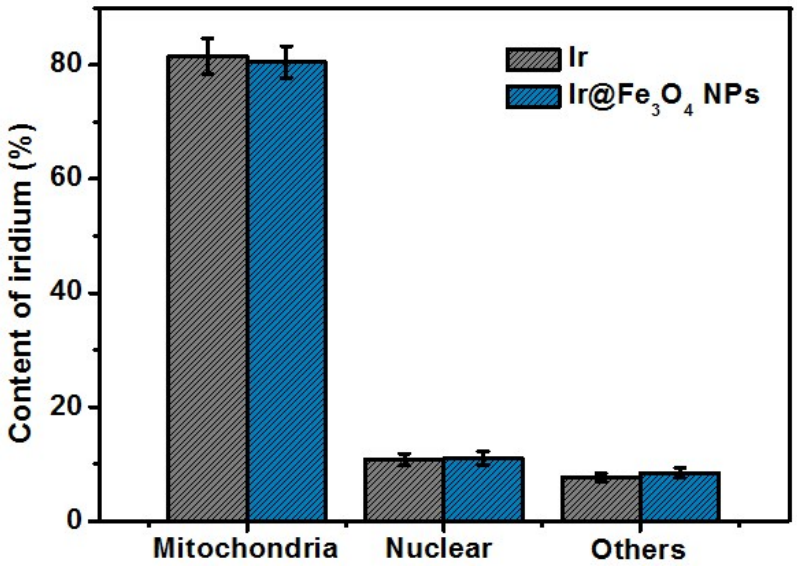

Fig. S14 The internalized iridium of the HeLa cells was quantified by ICP-MS. HeLa cells were treated with **Ir** or **Ir@Fe_3O_4 NPs** for 4 h. The mitochondria, nuclear and others were extracted using mitochondrial isolation and nuclear isolation kits.

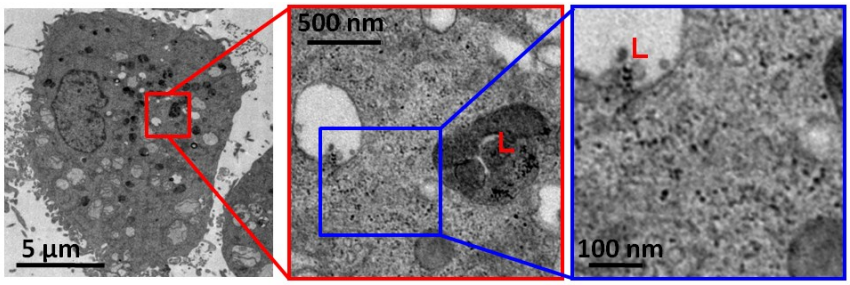

Fig. S15 Bio-TEM images of distribution of **Ir@Fe_3O_4 NPs** in HeLa cell (2 h). L: lysosome.

The particles escaped from the lysosome to cytoplasm.

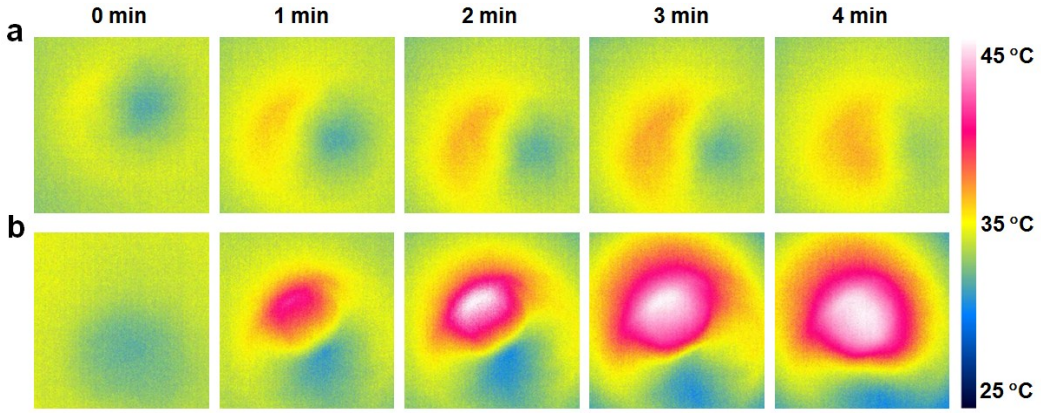

Fig. S16 IR thermal images of HeLa cells without (a) or with (b) **Ir@Fe_3O_4 NPs** treatment under exposure to the 808 nm laser.

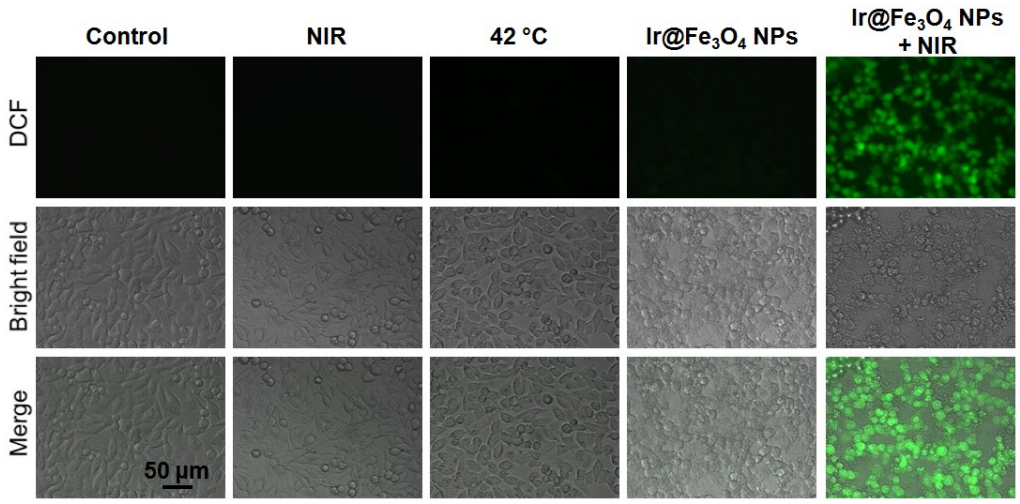

Fig. S17 Microscopic images of ROS levels in HeLa cells stained with DCFH-DA after the various treatments indicated.

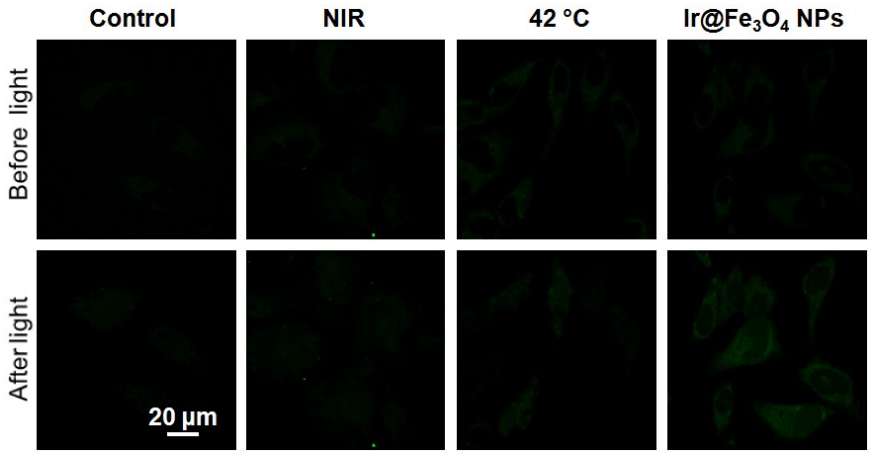

Fig. S18 Microscopic images of •OH generation in HeLa cells detected by HPF before and after various treatments indicated.

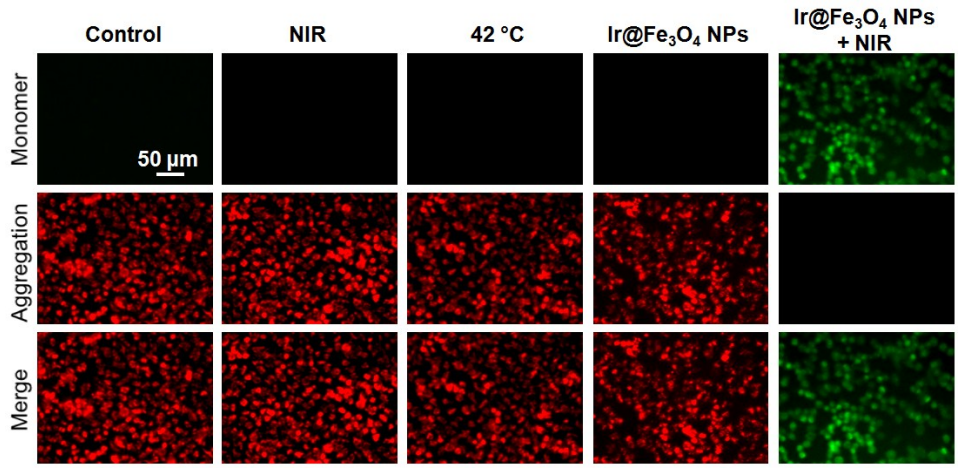

Fig. S19 Microscopic images of mitochondrial transmembrane potential (MMP) in HeLa cells stained by JC-1 after various treatments indicated.

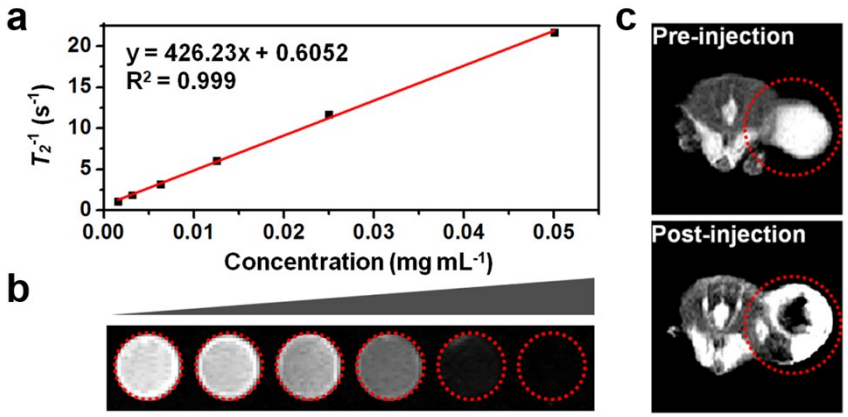

Fig. S20 (a) T_2 relaxation rates (r_2) and (b) T_2-weighted MR images of **Ir@Fe_3O_4 NPs** with different concentrations. (c) T_2-weighted MR images of HeLa tumor bearing mice before and after injection of **Ir@Fe_3O_4 NPs**.

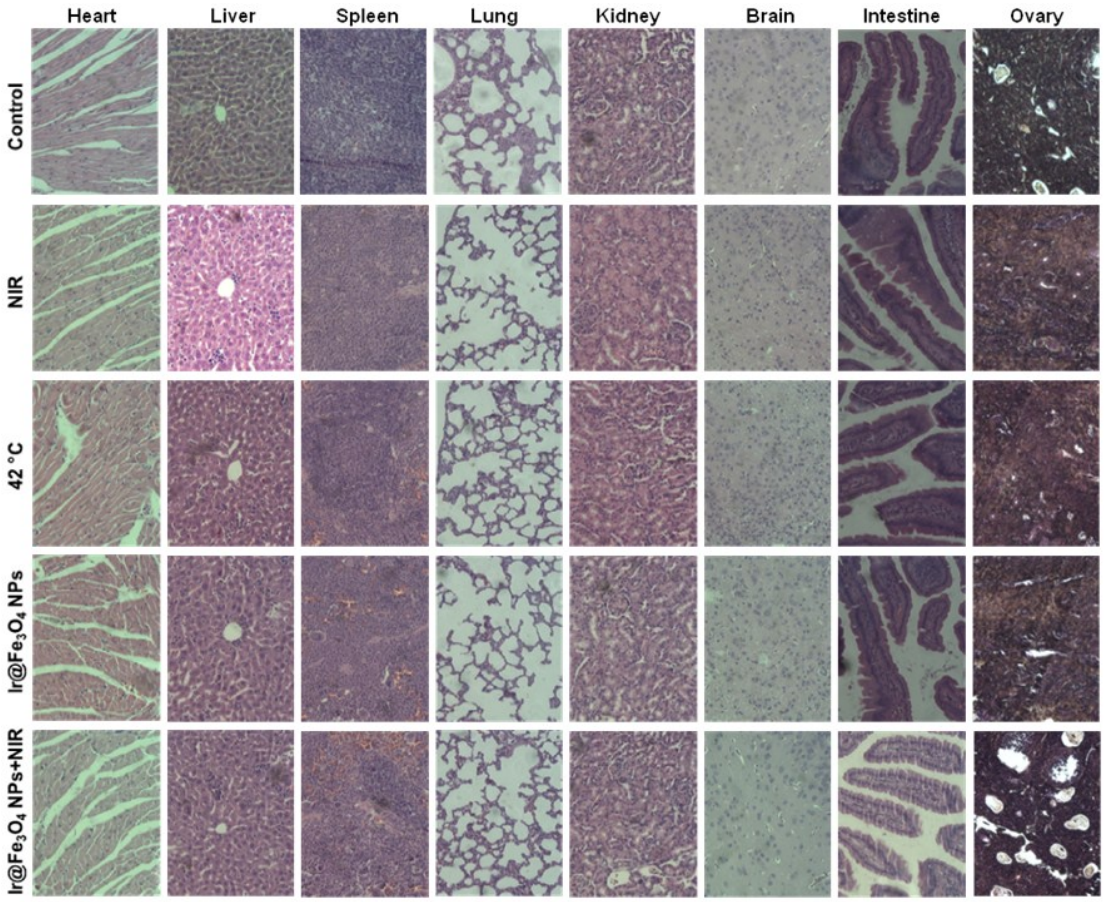

Fig. S21 Histological examination of primary organs (heart, liver, spleen, lung, kidney, brain, intestine and ovary) after various treatments indicated. Sections for light microscopy were stained with hematoxylin-eosin (H&E). Samples were from three different mice of the experiment. Magnification was 200×.

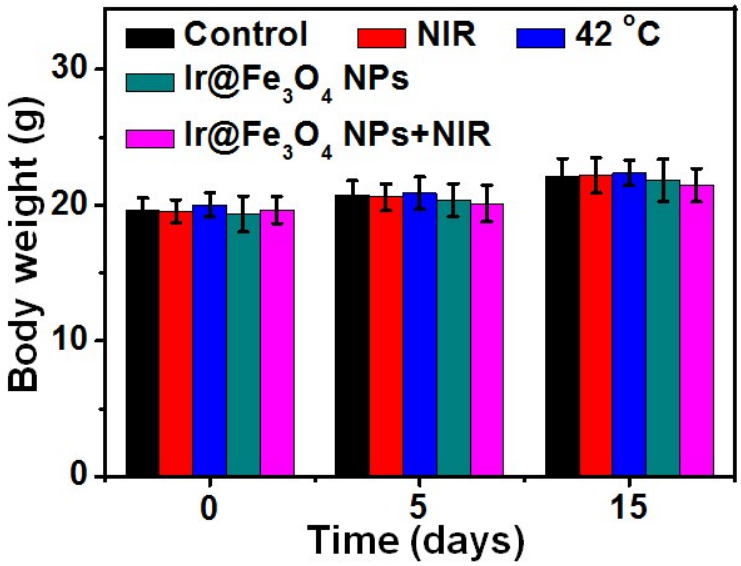

Fig. S22 Body weight changes with time of mice after various treatments indicated.